Thrust Magnitude and Efficiency Studies for Multiple Robotic Flapping Fins

Jason D. Geder and Ravi Ramamurti
Laboratories for Computational Physics and Fluid Dynamics
Naval Research Laboratory
Washington, DC 20375

Marius Pruessner
Center for Biomolecular Science and Engineering
Naval Research Laboratory
Washington, DC 20375

***Abstract*—The development of multiple generations of robotic flapping pectoral fins has warranted a closer study of the relative thrusts and efficiencies exhibited by these fins. This paper describes the differences between the various fins – including stroke frequency, stroke amplitude, aspect ratio, and effective angle of attack – and investigates the effects these differences have on thrust generation and propulsive efficiency. Drawing from and building on previous fin results, both computational fluid dynamics (CFD) simulation results and experimental data are used to evaluate the thrust, power draw, and efficiency, and to find useful relationships between these values and parameters such as Strouhal number and advance ratio. This analysis has implication for future fin design and development of reduced order models for flapping propulsion mechanisms.**

Keywords—bio-inspired robotics; pectoral fin; underwater propulsion; propulsive efficiency; Strouhal number

I. Introduction

Design and development of oscillating fins for underwater thrust generation has exploded over the past decade. Scientists and engineers seeking to expand the envelope of undersea vehicle operations are increasingly turning to fish and marine mammals to study the mechanisms that provide these creatures with superior maneuvering performance. However, as an exact copy of a fish fin or dolphin fluke cannot be made in the lab, understanding how the attributes and motions of the propulsion mechanism contribute to thrust enables effective design changes.

Various research groups have pursued the development of rigid and passively deforming fins [1]-[4], as well as some actively controlled curvature fins [5]-[7]. Biologists have studied the effects of fin shape and scaling on thrust [8][9], but on the engineering side, less research has been done to understand the influence of shape, size, and kinematics. More detailed studies on the thrust producing mechanisms in robotic fins would provide a useful design tool for future systems.

Adapting studies of the bird wrasse (*Gomphosus varius*) pectoral fin, four generations of actively controlled curvature robotic fins have been designed and built [5][10][11]. These fins have evolved based on thrust requirements, durability, and mission needs. Through the redesign processes, choices were made about fin size and geometry to address some mission requirements [11], although maximizing thrust and efficiency were not always the primary objectives of these efforts.

In this paper, we analyze the results from the four generations of fins to identify characteristics that lead to high thrust and efficiency over a range of flow speeds. Further, we quantify relationships between these performance metrics and two non-dimensional numbers used for describing oscillating mechanisms in a flow, Strouhal number and advance ratio.

II. Fin Designs

Based on studies of the bird wrasse pectoral fin geometry and kinematics, a first generation (Gen1) robotic fin was designed and built to retain the curvature control needed to achieve high thrust [5]. A scaled up second generation (Gen2) fin retaining the same planform shape as the Gen1 fin was designed to address vehicle speed and maneuvering requirements for a field operational vehicle [10]. More recently, third generation (Gen3a and Gen3b) fins were developed to address new mission requirements [11] and increase fin curvature limits. Design changes were made to the fin rib mechanisms, membrane material, planform shape, and size in order to obtain the Gen3a and Gen3b fins. The various fins are shown in Figure 1, illustrating these changes.

As the geometry, mechanisms, and materials changed, so did the kinematics of fin motion including amplitude, frequency, and surface curvature. Each successive fin demonstrated unique thrust time histories, but the exact characteristics leading to thrust differences have not been fully understood. Breaking down the fin motions into individual components will allow us to scale force and efficiency results by parameters other than just surface area or upstream flow velocity.

One of the notable differences between the fin kinematics is the limitation of stroke frequency and amplitude. The Gen3a fin, being the largest of the four fins (planform area = 435cm^2), has the most limited frequency-amplitude combination due to actuator dynamics and fin size. Another major difference is in fin shape and number of ribs. The Gen1 and Gen2 fins are relatively longer (higher aspect ratio) and have five spanwise directed ribs, while the Gen3a and Gen3b fins have a much shorter span-to-chord ratio and have four and three ribs, respectively. Further, the ribs on the Gen3a and Gen3b fins have a variable splay angle to conform to the fin membrane. Finally, the maximum bending of the fin ribs is different for each fin. The Gen3b fin allows for the most relative deflection of the four fins, while the Gen1 and Gen2 are the most limited due to rib design and membrane material.

U.S. Government work not protected by U.S. Copyright

This is a DRAFT. As such it may not be cited in other works.
The citable Proceedings of the Conference will be published in
IEEE Xplore shortly after the conclusion of the conference.

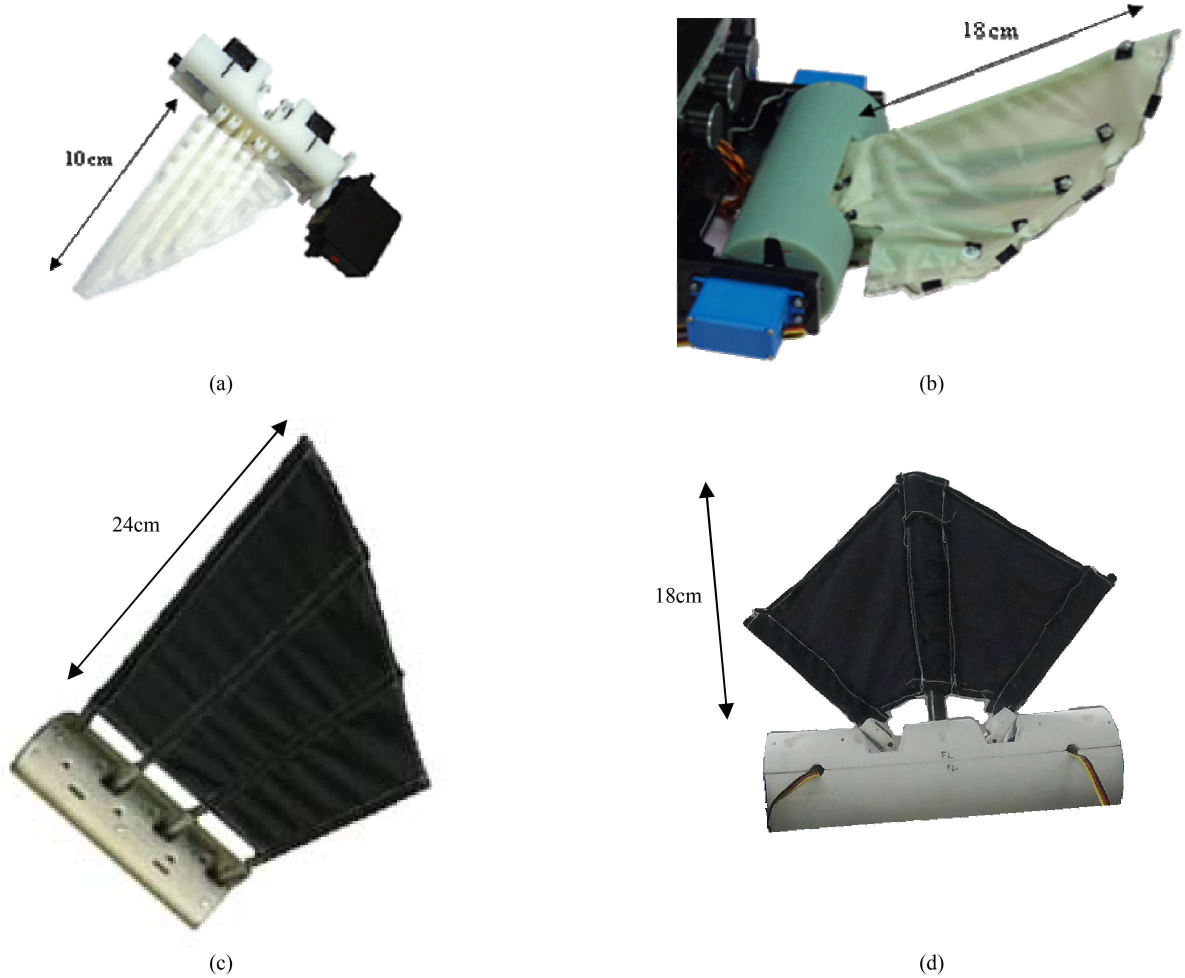

Fig. 1. (a) Gen1, (b) Gen2, (c) Gen3a, and (d) Gen3b fins developed for the vehicle, Wrasse-inspired Agile Near-shore Deformable-fin Automaton (WANDA).

III. Fin Thrust Time Histories

The bulk motion of the fin is due to a rotation of the fin about an axis parallel to the direction of motion. To generate positive thrust with each of the fins, a set of fin kinematics is programmed with the leading edge of the fin leading the up- and down-strokes. Further, the up- and down-strokes are roughly symmetric.

Fin thrust time histories at zero upstream flow speed for the Gen1, Gen2, and Gen3a fins are shown in Figure 2. In this study the Gen1 fin refers to Gen1 kinematics on a fin scaled up to the Gen2 size. While the Gen1 and Gen2 fins are much smaller than the Gen3a, we see that the time history in Figure 2a does not indicate a large difference in thrust generated by these fins throughout a stroke cycle. In fact, the five sets of fin kinematics studied yield a cycle-averaged thrust between 1.7N and 2.7N. However, looking at the coefficient of thrust (Eq. 1) we see a separation of the Gen1 and Gen2 curves from the Gen3a curves indicating a performance advantage not directly attributed to fin area or tip speed.

$$C_T = \frac{T}{\frac{1}{2}\rho {V_{ref}}^2 S_{fin}} \tag{1}$$

Here, C_T is the thrust coefficient, T is thrust magnitude, V_{ref} is the resultant velocity magnitude seen by the fin due to upstream flow and flapping velocities, and and S_{fin} is fin planform area. The Gen1 and Gen2 kinematics yield a mean thrust coefficient between C_T = 0.9 and C_T = 1.2, whereas the Gen3a kinematics yield C_T = 0.4. This difference must be due to some combination of fin geometry and curvature differences, as the Gen3a fin significantly deviated from earlier versions in shape and actuation.

One metric to quantify the difference between the Gen1-Gen2 fins and the Gen3a fin is in aspect ratio (AR) which is defined as,

$$AR = \frac{b^2}{S_{fin}} \tag{2}$$

where b is fin span. The Gen1 and Gen2 fins both have AR = 3.2, while the Gen3a fin has AR = 1.3. This factor of 2.5 difference has been shown to contribute to over 50% increase

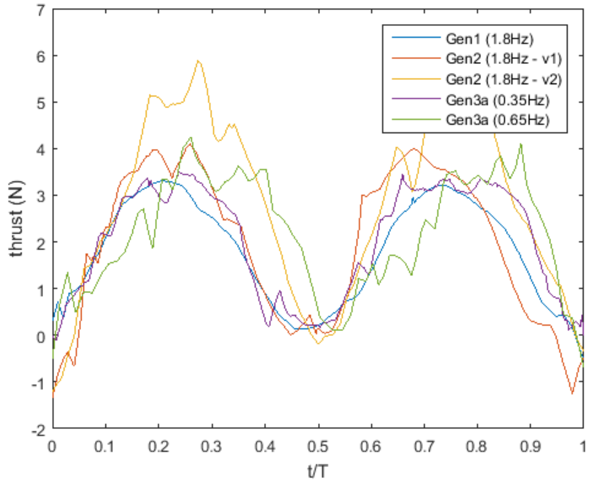

(a)

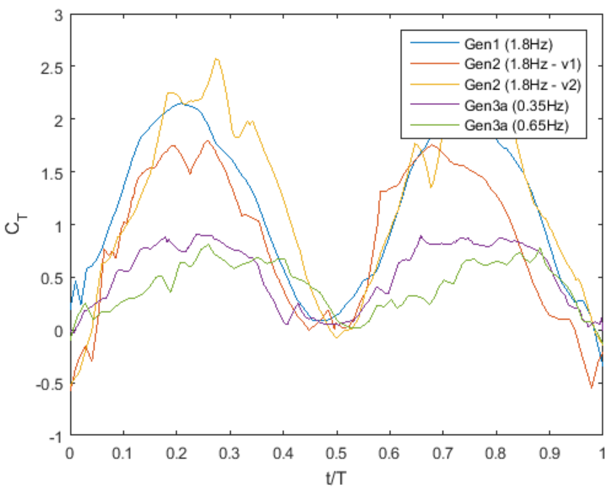

(b)

Fig. 2. (a) Thrust time history and (b) coefficient of thrust time history over a single stroke cycle for the Gen1, Gen2, and Gen3a fins at zero upstream flow speed.

in lift coefficient for relatively low aspect ratio lifting surfaces [12]. As the motion of our flapping fin generates thrust in a manner similar to how a wing creates lift, we can attribute a portion of the difference in C_T to aspect ratio.

A second metric to quantify the difference in C_T is the effective angle of attack (α) for the flapping fin. Lift and drag coefficients as functions of α vary depending on the lifting surface cross-section. In our case, the cross-section of the Gen1 and Gen2 fins (which have a tapered thickness that decreases from leading to trailing edge) is quite different from that of the Gen3a fin (which more resembles a flat plate cross-section). However, most lift slopes are negative for $\alpha > \sim 40°$ [13] and for flat plates C_L peaks between $\alpha = 25°$ and $\alpha = 45°$ [14][15]. During fin midstroke, when angle of attack is minimized and maximum thrust generated, the Gen3a fin is at $\alpha = 62°$ for 0.35 Hz flapping and $\alpha = 68°$ for 0.65Hz flapping. In contrast, the Gen1 fin is at $\alpha = 56°$, and the Gen2 fin is at $\alpha = 51°$ and $\alpha = 43°$ for its two sets of kinematics. It is reasonable to assume that both the Gen3a flat plate cross-section and higher angle of attack (above 40°) contribute to a lower thrust coefficient.

IV. Fin Thrust at Non-zero Speed

Experiments and simulation of the most recent iteration of the fin (Gen3b) has demonstrated not just the importance of chordwise fin curvature on thrust, but also its dependence on upstream flow speed, U_∞. By studying the thrust generated by this one iteration of the fin, we can hold AR, planform shape, and fin area constant, and focus on the effects of changing fin kinematics.

Controlling fin curvature through rotation of the ribs, we selected a few different curvatures to investigate. While the curvatures change throughout the stroke, they are defined by the chordwise cross-sectional shape at the 65% span location on the fin (Fig. 3). This location was chosen as it is the time-averaged center of pressure on the fin during the stroke. The 0.8 Hz and 1.6 Hz (v1) strokes maximize the relative rib deflections, thus maximizing the curvature. The 1.6 Hz (v2) stroke reduces both the leading edge and trailing edge tip deflections resulting in a much smaller fin curvature at midstroke. The 1.6 Hz (v3) stroke reduces the trailing edge rib

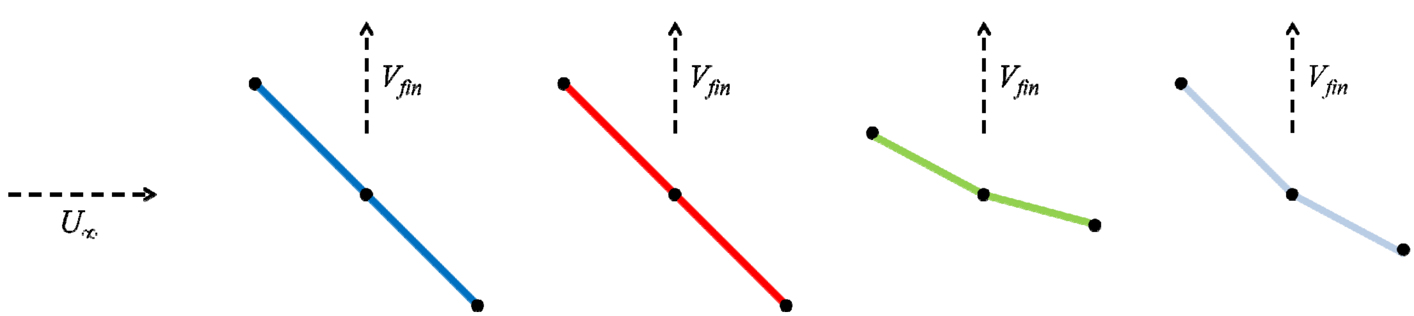

(a) (b) (c) (d)

Fig. 3. Cross-section of the Gen3b fin taken during midstroke for the kinematics at (a) 0.8Hz, (b) 1.6Hz, (c) 1.6Hz with reduced leading and trailing edge deflection, and (d) 1.6Hz with reduced trailing edge deflection.

deflection resulting in less curvature than the baseline (v1), but larger than the v2 stroke.

As we see in Figure 4a-b, the fin kinematics with higher average curvature produce significantly higher thrust and have higher thrust coefficients at $U_\infty = 0$ than the lower curvature variants. However, as inflow speed increases the thrust production of these high curvature fins decreases rapidly, while the thrust produced by the lower curvature fins demonstrates a much smaller decline in thrust production.

As upstream flow speed increases, not only does the effective flow speed over the fin increase, but the direction of the flow changes as well. Again, focusing on the midstroke as this is where most of the thrust is generated, Figure 4c shows the fin trailing edge angle of attack (α_{TE}) to the flow as a function of upstream flow speed. The trailing edge angle of attack is used as it takes into account the camber in the v2 and v3 kinematics, as well as the leading edge angle of attack.

At $U_\infty = 0$, the two high curvature kinematics have a midstroke $\alpha_{TE} \approx 40°$. Based on the studies of flat plate lift discussed earlier [14][15], this operating point could produce close to maximum thrust for the Gen3b fin at zero speed. The two lower curvature kinematics, v2 and v3, have much larger trailing edge angles of attack at $U_\infty = 0$ ($\alpha_{TE} = 75°$ and $\alpha_{TE} = 61°$, respectively). At these operating points, the thrust coefficient has decreased by a factor of 4-6 times.

As we increase speed to $U_\infty = 0.5$ m/s (1 kt), the angle of attack during midstroke has dropped below zero for the high curvature fins indicating that the thrust produced is actually in the negative direction. This is validated by the thrust produced by these kinematics at $U_\infty = 0.5$ m/s. In contrast, the lower curvature kinematics maintain a positive angle of attack, and also positive thrust at $U_\infty = 0.5$ m/s. Finally, moving to $U_\infty = 1.0$ m/s, the only kinematics that maintains a positive angle of attack during midstroke is the only kinematics that produces positive thrust at this speed.

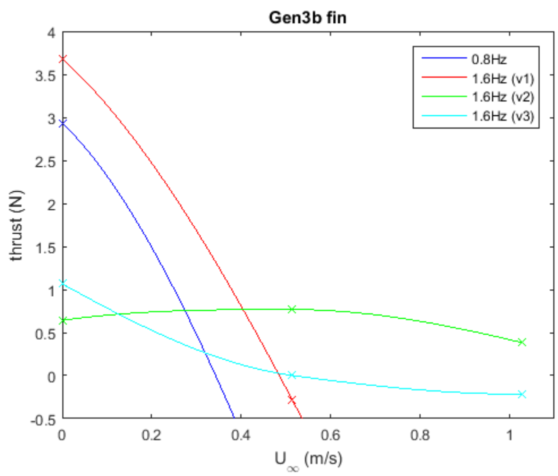

(a)

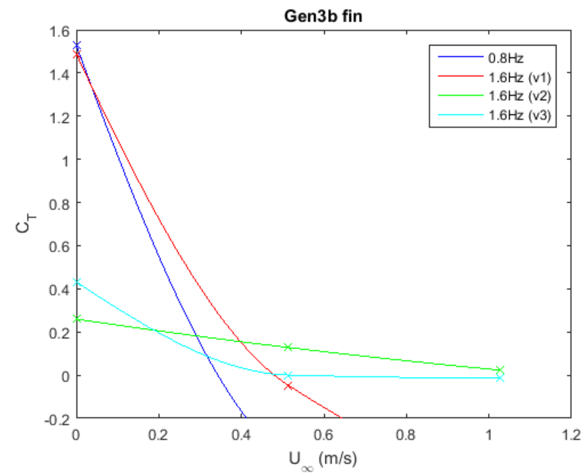

(b)

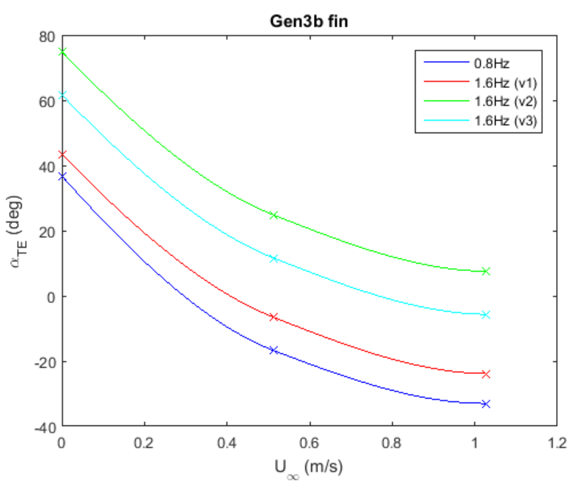

(c)

Fig. 4. (a) Average thrust, (b) average thrust coefficient, and (c) fin angle of attack for the Gen3b fin at various inflow speeds, U_∞, showing that the v2 and v3 produce lower thrust at low speeds, but higher thrust at high speeds.

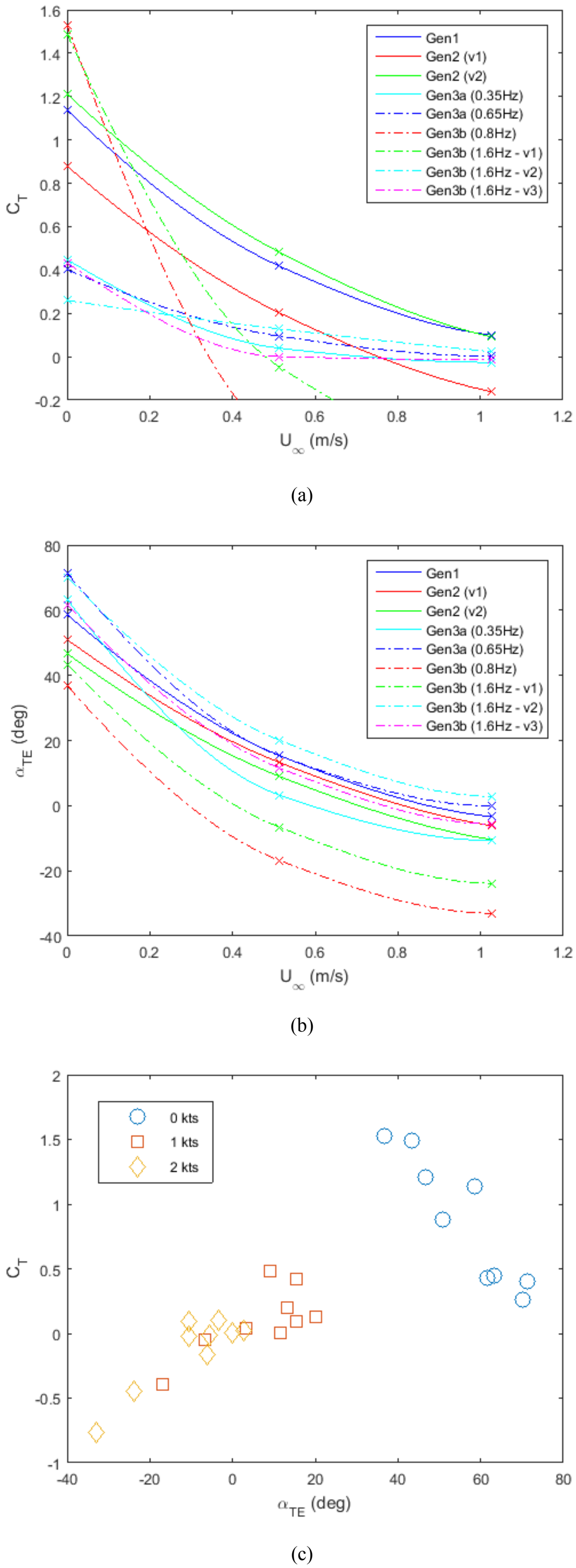

Fig. 5. (a) Average thrust coefficient and (b) fin angle of attack at various inflow speeds, U_∞, for all fin generations. (c) Thrust coefficient as a function of fin angle of attack, grouped into upstream flow speeds.

Moving to a comparison of all fin generations tested, we see a similar trend in relative C_T for each of the fins as a function of upstream flow speed and fin angle of attack (Fig. 5). Clustering the points in a C_T versus α_{TE} plot by upstream flow speed (Fig. 5c), there is a clear trend showing maximum C_T moving towards the $\alpha_{TE} = 20°$ to $\alpha_{TE} = 40°$ window. This corresponds to optimal angles of attack for flat plate lift production [15].

A common non-dimensional value used for describing oscillating flow systems is Strouhal number which gives a ratio of oscillation speed to external flow speed (Eq. 3).

$$St_{V_{ref}} = \frac{f \cdot (\theta_{TE} \cdot b_{TE})}{V_{ref}} \tag{3}$$

For the fins, we define St_{Vref} as the Strouhal number, f as the fin flapping frequency, θ_{TE} as stroke amplitude of the trailing edge, and b_{TE} as the spanwise length of the trailing edge.

Using Strouhal number to evaluate thrust, we see an inverse relationship (Fig. 6), which is expected since U_∞ is in the denominator of *St*. Also, similar to the plot of C_T versus U_∞, the slope magnitude is highest for the Gen3b fin, while it is smallest for the Gen3a fin.

V. Propulsive Efficiency

Computationally, we extract the hydrodynamic efficiency by computing thrust, speed, and hydrodynamic power. Experimentally, instead of hydrodynamic power, we measure total power consumption to get overall propulsive efficiency (Eq. 4), and by subtracting hydrodynamic power, we can get mechanical and other losses in the system.

$$\eta_\infty = \frac{T \cdot U_\infty}{P_{in}} \tag{4}$$

Here, η_∞ is the propulsive efficiency, T is fin thrust and P_{in} is the power expended to flap the fins. While the data collected in this study is limited to measurements at U_∞ equal to 0.0, 0.5, and 1.0 m/s, it is clear that the maximum propulsive efficiency is somewhere close to U_∞ = 0.5m/s for most iterations of the

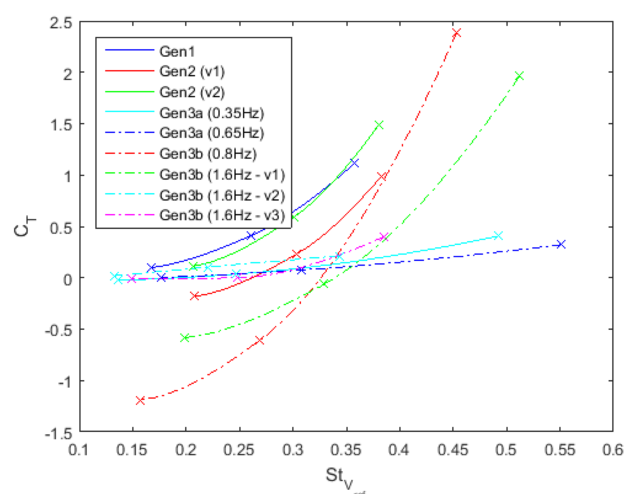

Fig. 6. Thrust coefficient as a function of Strouhal number for all fin generations.

fin (Fig. 7a). This maximum efficiency, or cruise, speed skews slightly higher for the Gen1 and Gen2 fins. As discussed in the previous section, these generations of the fin maintained higher thrust coefficients than Gen 3a and Gen3b fins at higher speeds, and they did so without much additional power consumption.

In nature, fish and other aquatic organisms have exhibited optimal propulsive efficiencies in the range of St = 0.2 to St = 0.4 [16][17]. Computationally, higher Strouhal numbers closer to St = 0.5 have also yielded maximum efficiency [18]. The results of this study are in the same range as previous studies. For all fins, a Strouhal number between 0.15 and 0.35 yielded the highest propulsive efficiency (Fig. 7b). For the Gen1 and Gen2 fins, the maximum efficiency occurred towards the lower end of this range, while for the Gen3a fin it was towards the higher end.

Another non-dimensional parameter that can be used for characterizing oscillating systems is advance ratio which gives a ratio of the distance traveled by the fin tip and the spanwise length of the fin (Eq. 5).

$$J = \frac{U_\infty}{V_{tip}} \quad (5)$$

Here, J is the advance ratio and V_{tip} is the fin tip speed. [19] showed that pectoral fin swimmers swim over a wide range of advance ratios from J = 0.2 to J = 1.8, generally dependent on swimming speed. In this study, the fins have a maximum propulsive efficiency at advance ratios between J = 0.8 and J = 1.8 (Fig. 7c) depending on the fin and kinematics.

VI. Discussion and Conclusions

The results of this study have served to characterize the previously developed fins, and also have implications for optimizing the selection or development of fins for various operating speeds.

Thrust results indicated that higher aspect ratio fins performed better in thrust production, and that we should strive to maintain an optimal stroke angle of attack ($\alpha_{TE} \approx 40°$) as upstream flow speeds change. Generally, this means that as flow speed increases, fin midstroke curvature must decrease. For the fins we have built, the Gen1 and Gen2 fins generally performed better in thrust at higher speeds because of their relatively high aspect ratios and smaller natural curvature due to limited rib motion. In efficiency, the Gen1 and Gen2 fins also performed better at higher speeds due to similar or lower power consumption compared to the Gen3a and Gen3b fins. At lower speeds, the later generation fins performed better, and when the curvature of these fins was reduced (Gen3b, v2 and v3), higher speed efficiency also improves.

While a clear relationship was discovered between fin thrust at a given speed and trailing edge angle of attack, it is impossible to formulate an analytical equation quantifying this relationship without better data on the T versus α_{TE} curves for specific low aspect ratio fin geometries at high angles of attack. A detailed study for various geometries could provide a database to quantify this relationship, and get closer to converging the C_T curves for different fins. Even without an explicit equation for this relationship, the results for

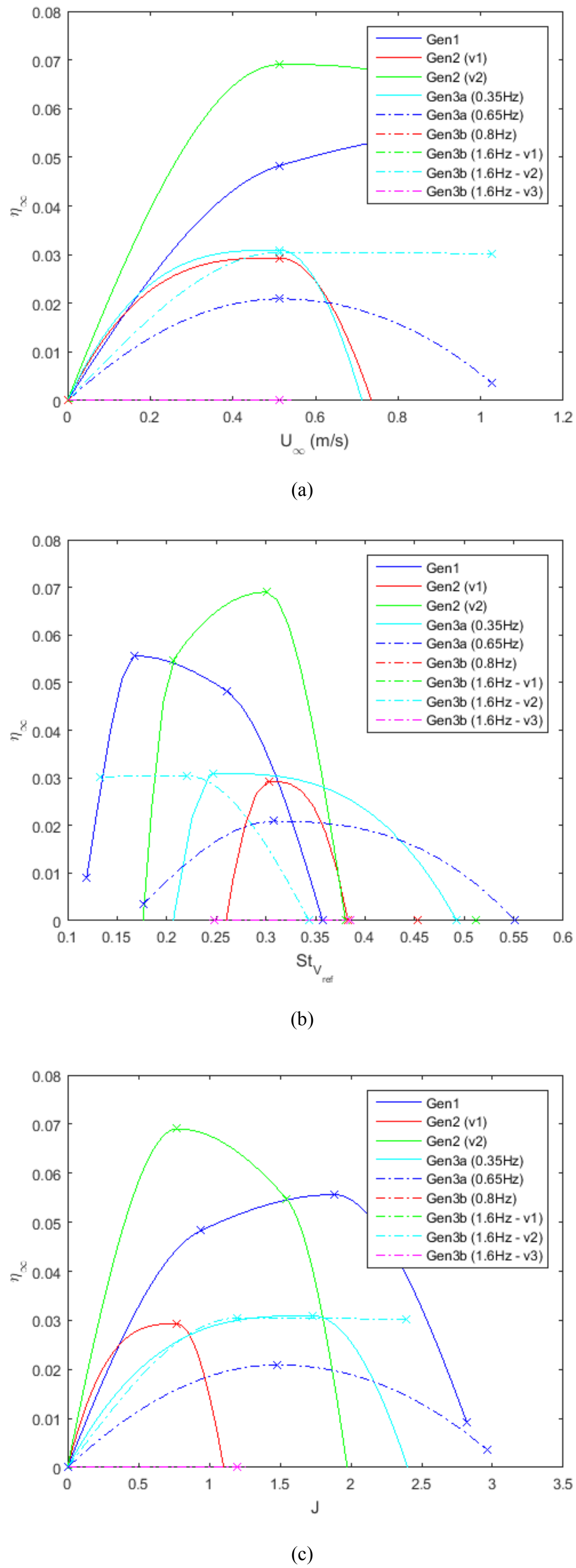

Fig. 7. Propulsive efficiency for all fin generations as functions of (a) upstream flow speed, (b) Strouhal number, and (c) advance ratio.

maximizing C_T for a given upstream flow speed based on angle of attack are useful for designing speed dependent fin kinematics for a given fin configuration.

Beyond characterization of fin thrust as a function of size, stroke frequency, stroke amplitude, aspect ratio, and angle of attack, an analysis of useful non-dimensional flow parameters identified common fin operating points. The results demonstrating a range of Strouhal numbers and advance ratios for which the fins exhibit maximum efficiency can be used as a metric in the design of future fins and flapping kinematics. They can also be useful in the development of reduced order models of flapping fin systems.

References

[1] B. Hobson, M. Murray, and C. A. Pell, "PilotFish: Maximizing agility in an unmanned underwater vehicle", proceedings of the International Symposium on Unmanned Untethered Submersible Technology, Durham, NH, 1999.

[2] S. Licht, V. Polidoro, M. Flores, F. S. Hover, and M. S. Triantafyllou, "Design and projected performance of a flapping foil AUV", IEEE Journal of Oceanic Engineering, vol. 29, no. 3, pp. 786-794, 2004.

[3] P. Sitorus, Y. Nazaruddin, E. Leksono, and A. Budiyono, "Design and implementation of paired pectoral fins locomotion of labriform fish applied to a fish robot", Journal of Bionic Engineering, vol. 6, pp. 37-45, 2009.

[4] N. Kato, et al., "Elastic pectoral fin actuators for biomimetic underwater vehicles", in Bio-mechanisms of Swimming and Flying, chap. 9, Springer Japan, pp. 271-282, 2008.

[5] J. Palmisano et al., "Design of a biomimetic controlled-curvature robotic pectoral fin", proceedings of IEEE Int. Conf. on Robotics and Automation, Rome, Italy, 2007.

[6] K. W. Moored, W. Smith, W. Chang, and H. Bart-Smith, "Investigating the thrust production of a myliobatoid-inspired oscillating wing", proceedings of the 3rd International CIMTEC Conference, Acireale, Italy, June 2008.

[7] J. Tangorra et al., "The effect of fin ray flexural rigidity on the propulsive forces generated by a biorobotic fish pectoral fin", Journal of Experimental Biology, vol. 213, pp. 4043-4054, 2010.

[8] R.W. Blake, "Influence of pectoral fin shape on thrust and drag in labriform locomotion", Journal of Zoology, vol. 194, no. 1, pp. 53-66, 1981.

[9] T.L. Daniel, "Unsteady Aspects of Aquatic Locomotion", American Zoologist, vol. 24, no. 1, pp. 121-134, 1984.

[10] J. D. Geder et al., "Scaling studies for an actively controlled curvature robotic pectoral fin", International Conference on Intelligent Robotics and Applications, pp. 141-150, Montreal, Canada, November 2012.

[11] J. D. Geder et al., "Development of a Robotic Fin for Hydrodynamic Propulsion and Aerodynamic Control", proceedings of the MTS/IEEE OCEANS14, St. Johns, Newfoundland, Canada, September 2014.

[12] A. Filippone and M.S. Selig, "Low-Aspect-Ratio Wings for Wing-Ships", 36th AIAA Aerospace Sciences Meeting, Reno, NV, January 1998.

[13] R.E. Sheldahl and P.C. Klimas, "Aerodynamic Characteristics of Seven Symmetrical Airfoil Sections Through 180-Degree Angle of Attack for Use in Aerodynamics Analysis of Vertical Axis Wind Turbines", Sandia National Laboratories Energy Report, SAND80-2114, March 1981.

[14] X. Ortiz, D. Rival, and D. Wood, "Forces and Moments on Flat Plates of Small Aspect Ratio with Application to PV Wind Loads and Small Wind Turbine Blades", Energies, vol. 8, pp. 2438-2453, 2015.

[15] J.D. Holmes, C.W. Letchford, and N. Lin. "Investigations of plate-type windborne debris—Part II: Computed trajectories", Journal of Wind Eng. Ind. Aerodyn., no. 94, pp. 21–39, 2006.

[16] G.K. Taylor, R.L. Nudds, and A.L.R. Thomas, "Flying and swimming animals cruise at a Strouhal number tuned for high power efficiency", Nature, vol. 425, pp. 707-711, 2003.

[17] K. Shoele and Q. Zhu, "Numerical simulation of a pectoral fin during labriform swimming", Journal of Experimental Biology, vol. 213, pp. 2038-2047, 2010.

[18] M. Bozkurttas, J. Tangorra, G. Lauder, and R. Mittal, "Understanding the Hydrodynamics of Swimming: From Fish Fins to Flexible Propulsors for Autonomous Underwater Vehicles", Advances in Science and Technology, vol. 58, pp. 193-202, 2008.

[19] M.E. Hale, R.D. Daly, D.H. Thorsen, and M.W. Westneat, "Pectoral fin coordination and gait transitions in steadily swimming juvenile reef fishes", Journal of Experimental Biology, vol. 209, pp. 3708-3718, 2006.